Mitochondrial matrix protein Letmd1 maintains thermogenic capacity of brown adipose tissue

Anna Park
KRIBB https://orcid.org/0000-0002-7323-9114
Kwang-eun Kim
Korea Advanced Institute of Science and Technology https://orcid.org/0000-0002-5355-1979
Isaac Park
Seoul National University
Dae-Soo Kim
Kribb https://orcid.org/0000-0002-4999-1613
Jaehoon Kim
KAIST
Dae-Sik Lim
Korea Advanced Institute of Science and Technology https://orcid.org/0000-0003-2356-7555
Euijeon Woo
Korea Research Institute of Bioscience and Biotechnology https://orcid.org/0000-0001-6983-0270
Eun-Woo Lee
Korea Research Institute of Bioscience and Biotechnology (KRIBB) https://orcid.org/0000-0002-5156-0003
Baek-Soo Han
Korea Research Institute of Bioscience and Biotechnology
Kyoung-Jin Oh
Korea Research Institute of Bioscience and Biotechnology (KRIBB) https://orcid.org/0000-0002-2224-7202
Sang Chul Lee
Korea Research Institute of Bioscience and Biotechnology (KRIBB)
Ji Young Mun
Korea Brain Research Institute
Hyun-Woo Rhee
Seoul National University https://orcid.org/0000-0002-3817-3455
Won Kon Kim
Korea Research Institute of Bioscience and Biotechnology (KRIBB) https://orcid.org/0000-0002-1289-0333
Kwang-Hee Bae

Metabolic Regulation Research Center, Korea Research Institute of Bioscience and Biotechnology (KRIBB) https://orcid.org/0000-0002-5868-2556

Jae Myoung Suh (jmsuh@kaist.ac.kr)

Korea Advanced Institute of Science and Technology https://orcid.org/0000-0001-8097-4662

Article

Keywords: Letmd1, OXPHOS, Mitochondria, Mitochondrial matrix, Mitochondria dysfunction, Brown adipose tissue, Ucp1, Thermogenesis, Topology, APEX2

Posted Date: November 15th, 2021

DOI: https://doi.org/10.21203/rs.3.rs-1046884/v1

Version of Record: A version of this preprint was published at Nature Communications on June 23rd, 2023. See the published version at https://doi.org/10.1038/s41467-023-39106-z.

Abstract

Brown adipose tissue (BAT) has abundant mitochondria with the unique capability of generating heat via uncoupled respiration. Mitochondrial uncoupling protein 1 (Ucp1) is activated in BAT during cold stress and dissipates mitochondrial proton motive force generated by the electron transport chain to generate heat. However, other mitochondrial factors required for brown adipocyte respiration and thermogenesis under cold stress are largely unknown. Here we identify LETM1 domain-containing protein 1 (Letmd1) is a BAT-enriched, cold-induced protein that is required for cold-stimulated respiration and thermogenesis of BAT. Proximity labeling studies reveal that Letmd1 is a mitochondrial matrix protein. Letmd1 knockout mice display aberrant BAT mitochondria and fail to carry out adaptive thermogenesis under cold stress. Letmd1 knockout BAT is deficient in oxidative phosphorylation (OXPHOS) complex proteins and has impaired mitochondrial respiration. Taken together, we identify that the BAT-enriched mitochondrial matrix protein Letmd1 is required for cold-stimulated respiration and thermogenic function of BAT.

Introduction

Brown adipose tissue (BAT) differs from white adipose tissue (WAT) in that BAT is highly responsive to cold exposure for adaptive thermogenesis. BAT has abundant mitochondria that carry out its unique heat-generating function. Uncoupling protein 1 (Ucp1), localized to the mitochondrial inner membrane of brown adipocytes, plays a major role in the thermogenic function of brown adipocytes. When BAT is activated by cold conditions, Ucp1 dissipates proton (H+) motive force in the form of heat as a transporter of protons generated by the mitochondrial respiratory chain (Klingenberg, 1990). In this respect, mitochondrial respiration in BAT has an essential role in regulating whole-body energy homeostasis through adaptive thermogenesis in cold stress.

BAT glucose uptake and mitochondrial oxidative activity is increased by cold exposure in rodents (Labbé et al., 2015) and humans (Blondin et al., 2014). In activated BAT, a coordinate increase in aerobic energy metabolism and UCP1-mediated uncoupled respiration metabolize nutrients for heat production in non-shivering thermogenesis. BAT transplantation improves glucose tolerance and insulin resistance (Stanford et al., 2013) and counteracts obesity in mice (Liu et al., 2015). Furthermore, in humans, BAT activation increases energy expenditure, reduces body fat mass, improves whole-body glucose disposal and insulin sensitivity (Yoneshiro et al., 2013, Chondronikola et al., 2014). Thus, therapeutic manipulation of BAT activity has emerged as a promising strategy for the treatment of obesity and metabolic disorders (Chechi et al., 2014, Saito et al., 2014). To successfully implement this strategy, it is crucial to understand the molecular components that mediate the cold response in BAT mitochondria. However, aside from UCP1, other BAT mitochondrial factors required for uncoupled respiration and thermogenesis under cold stress are largely unknown.

In this study, we surveyed cold-inducible mitochondrial proteins in BAT and identified LETM1 domain-containing protein1 (Letmd1) as a BAT-enriched factor that is localized to the mitochondrial matrix of brown adipocytes. Analysis of Letmd1 knockout mice revealed an essential role for Letmd1 in cold-

stimulated respiration and adaptive thermogenesis of BAT. Letmd1-deficient brown adipocytes show marked deficiency in oxidative phosphorylation (OXPHOS) complexes and dysmorphic mitochondrial ultrastructure. Elucidating the role of Letmd1 in BAT thermogenesis contributes to a deeper understanding of molecular mechanisms that enable the functional specialization of mitochondria in thermogenic BAT.

Results

Identification of cold-inducible mitochondrial proteins in brown adipose tissue

To identify candidate genes involved in the thermogenic function of BAT mitochondria, we analyzed publicly available gene expression data for genes that are enriched in BAT, as compared to epididymal WAT (eWAT) (GSE92844, (Mo et al., 2017)), and induced by cold stimulus (GSE70437, (Marcher et al., 2015)) **(Fig. S1A)**. From this analysis, we identified a cluster of 144 genes that were both enriched in BAT and induced by cold stimulation **(Fig. S1A)**. Among these 144 genes, we identified a subgroup of 31 genes which were annotated as mitochondrial genes including *Ucp1* **(Fig. S1B, Table S1)**.

Mitochondrial gene transcript levels and protein levels are frequently discordant, so we performed a complementary analysis with proteomics data (Forner et al., 2009). By analyzing the intersection of proteins that are BAT-enriched proteins and also induced by cold, 26 mitochondrial proteins were identified **(Fig. S1C, Table S1)**. After combining the results of the transcriptomic and proteomic analyses, three candidates, Ucp1, Letmd1, and Acsl5 were identified **(Fig. S1D)**. Ucp1 is a well-established mitochondrial protein required for BAT thermogenesis and Acsl5 has also been identified as an important regulator of whole-body energy metabolism in previous studies (Bowman et al., 2016). However, in contrast to these two genes, the role of Letmd1 in BAT has not been explored.

Letmd1 is a BAT-enriched protein that is upregulated in response to thermogenic demand

To begin to understand the role of Letmd1 in BAT, we examined Letmd1 expression during brown adipocyte differentiation in an immortalized brown preadipocyte (iBPA) cell culture model (Uldry M. et al., 2006). During iBPA differentiation into brown adipocytes, Letmd1 expression increased at both RNA and protein levels (Figs. 1A and 1B). In adult mice, Letmd1 protein was highly enriched in BAT relative to WAT and other tissues, including mitochondria-rich muscle, indicating that tissue mitochondrial content is not a determinant of Letmd1 expression levels (Fig. 1C). Thermogenic demand is known to increase during the early postnatal period of mice and we found that Letmd1 transcript and protein levels increased during this period (Figs. 1D and 1E).

We next compared Letmd1 expression in BAT from mice housed at thermoneutrality (30°C), room temperature (23°C), or cold (6°C) conditions and observed an inverse relationship between BAT Letmd1

expression and ambient temperature (Figs. 1F and 1G). Notably, when cold-exposed mice were re-acclimated to room temperature (Figs. 1H and 1I), cold-induced expression of Letmd1 reverted to room temperature levels (Fig. 1J), a pattern also seen for Ucp1 expression (Fig. 1K). Taken together, Letmd1 is enriched in mature brown adipocytes and shows dynamic regulation as a function of external cues determining the physiological demand for BAT thermogenesis.

Letmd1 is an integral membrane protein that targets to the mitochondrial matrix

Next, we investigated the subcellular localization of LETMD1 protein in brown adipocytes. Sequence analysis with MitoFates (Fukasawa et al., 2015) identified a putative mitochondrial targeting sequence (MTS) (1-28aa) and a cleavage site by mitochondrial processing peptidases (MPP) (Fig. 2A). In agreement with sequence analysis, immunofluorescence imaging of LETMD1 overexpressing iBPA cells displayed a mitochondrial pattern of localization (Fig. 2B). In addition to a mitochondrial presequence, LETMD1 protein contains two putative transmembrane domains (82-97aa and 139-161aa) as predicted by TMHMM analysis (Krogh et al., 2001) (Fig. 2C).

To gain more information on the domain structure and cellular localization of Letmd1 protein, we analyzed the activity of a series of APEX2 fusion expression constructs. APEX2 is an engineered peroxidase whose subcellular localization is visualized by electron microscopy (EM) of staining patterns generated by peroxidase activity (Martell et al., 2012). High resolution details offered by EM analysis of APEX2 staining patterns has been successful for determining mitochondrial compartment-specific localization and protein domain topology (Rhee et al., 2013, Hung et al., 2014, Hung et al., 2017, Lee et al., 2017) (Fig. 2D). EM imaging of HEK293 cells transfected with Letmd1-APEX2 (C-terminus APEX fusion) and APEX2-Letmd1 (N-terminus fusion) expression constructs both showed matrix staining patterns indicating that the N-terminus and C-terminus of Letmd1 are exposed to the matrix (Fig. 2E). While we observed a typical mitochondrial matrix pattern of peroxidase staining in cells expressing MTS-APEX2, APEX2 with an N-terminus mitochondrial targeting sequence (MTS), cells expressing the Letmd1-APEX2 construct lacking the predicted MTS (1-28aa) abolished mitochondrial localization demonstrating functionality of the Letmd1 MTS (Fig. 2E).

In another approach, we utilized the proximity labeling activity of a mitochondrial matrix localized APEX2, Matrix-APEX2, to test whether Letmd1 contains a matrix localized domain. To this end, iBPA cells were transfected with Matrix-APEX2 and Letmd1 expressing vectors. Letmd1 protein was detected in the biotin-labeled fraction of cell lysates indicating matrix localization of Letmd1 protein (Fig. 2F). These results were further confirmed *in vivo* as endogenous Letmd1 protein was detected in the labeled fraction of BAT lysates from Matrix-APEX2 transgenic mice which harbor a Matrix-APEX2 transgene under the control of a general promoter (Park et al., 2021) (Fig. 2G). These results demonstrate that Letmd1 is a mitochondrial matrix protein that contains a functional N-terminal MTS and two transmembrane domains spanning the inner mitochondrial membrane (Fig. 2H).

Letmd1 is required for adaptive thermogenesis

To study the *in vivo* function of Letmd1, we generated *Letmd1* knockout (KO) mice that are homozygous for a *Letmd1* null allele. Compared to control mice, *Letmd1* KO mice had increased body weight (Fig. 3A) in the absence of significant changes in food intake or physical activity (Figs. 3B and 3C). Gross examination of Letmd1 KO BAT tissue revealed a striking “whitened” appearance and histological analysis revealed dramatically enlarged lipid droplets in *Letmd1* KO BAT compared to littermate controls (Fig. 3D). Furthermore, the expression of Ucp1 and thermogenic genes were markedly reduced in *Letmd1* KO BAT from adult mice (Figs. 3E and 3F). This reduction in Ucp1 protein levels in *Letmd1* KO BAT was observed immediately after birth and persists through the perinatal period when thermogenic demand first arises (Fig. 3G). These findings led us to test whether thermogenic function of BAT is altered in *Letmd1* KO mice. Indeed, we found *Letmd1* KO mice failed to maintain core body temperature during a cold challenge indicating a defect in adaptive thermogenesis (Fig. 3H). Infrared imaging of *Letmd1* KO mice further confirmed the inability of *Letmd1* KO mice to activate BAT and maintain body temperature during a cold challenge (Fig. 3I).

To further characterize physiological alterations in *Letmd1* KO mice, we performed indirect calorimetry of control and *Letmd1* KO mice during a cold challenge. At 25 ℃, we did not observe any difference in oxygen consumption (VO_2) and carbon dioxide production (VCO_2) between the groups. However, while both wild-type and *Letmd1* KO mice rapidly increased VO_2 and VCO_2 upon initiation of a cold challenge, *Letmd1* KO mice failed to maintain elevated levels of VO_2 and VCO_2 which is necessary for a sustained thermogenic response (Figs. 3J and 3K). This impaired response to cold stress in *Letmd1* KO mice was accompanied by a failure to upregulate Ucp1 protein in BAT tissue (Fig. 3L). These results demonstrate an obligate *in vivo* requirement for Letmd1 function in the adaptive thermogenic response of BAT upon a cold challenge.

Letmd1 plays an essential role in maintaining BAT mitochondrial structure and respiratory function

To investigate the molecular role of Letmd1 in brown adipocyte function and adaptive thermogenesis, we performed RNA-seq analysis of *Letmd1* KO and wild-type BAT. Gene ontology (GO) analysis of transcriptome changes revealed down-regulation of a broad array of genes involved in processes that occur in the mitochondrial matrix compartment in *Letmd1* KO BAT (Fig. 4A). At the ultrastructural level, *Letmd1* KO BAT contained dysmorphic mitochondria with sparse distended cristae, a principal site of OXPHOS complex (Fig. 4B). These data led us to directly examine OXPHOS complex components and function in Letmd1 KO BAT. At embryonic day 16.5, when thermogenic demand is absent, BAT OXPHOS complex proteins were unaffected by Letmd1 deficiency (Fig. 4C). However, during the early postnatal period, control BAT upregulated OXPHOS complex proteins in response to thermogenic demand but *Letmd1* KO BAT failed to upregulate OXPHOS proteins during this critical period for BAT thermogenesis

(Fig. 4D). The defective OXPHOS protein expression in *Letmd1* KO BAT was further exacerbated in adult stages and showed a near complete loss of complex I and IV proteins (Fig. 4E).

To examine the functional consequence of OXPHOS complex deficiency in *Letmd1* KO BAT, we measured respiratory function in scrambled control (SCR) and *Letmd1* knockdown brown adipocytes (shLetmd1) in the presence or absence of isoproterenol stimulation. In the unstimulated state, we did not observe any significant differences in cellular respiration between SCR and shLetmd1 brown adipocytes (Figs. 4F and 4G). However, upon isoproterenol stimulation, we observed a dramatic reduction in maximal respiration of shLetmd1 cells, which is in sharp contrast with control (SCR) cells (Figs. 4F and 4G). Collectively, these data demonstrate a crucial role for Letmd1 in supporting brown adipocyte OXPHOS function in a stimulation-dependent manner.

Discussion

Adaptive thermogenesis of BAT is critical for defending against cold stress and maintaining body temperature in mammals. Mitochondrial protein Ucp1 plays a key role in this process by uncoupling ATP production from proton motive force generated by OXPHOS complexes. However, other than Ucp1, additional mitochondrial factors required for BAT thermogenesis are largely unknown. In this study, we uncover an essential role for the BAT-enriched protein Letmd1 in mitochondrial respiration and adaptive thermogenesis.

Letmd1 is annotated as a mitochondrial protein in MitoCarta 1.0 (Pagliarini et al., 2008), MitoCarta 2.0 (Calvo et al., 2016) and MitoCarta 3.0 (Rath et al., 2021). However, Letmd1 was categorized as one of the mitochondrial uncharacterized proteins (MXPs) in humans (Floyd et al., 2016) and the molecular and physiological function of Letmd1 in BAT has not been explored. Here, we demonstrate that Letmd1 has critical functions in regulating mitochondrial respiration to sustain BAT activation during adaptive thermogenesis.

Our proximity labeling enzyme-assisted topology studies identify Letmd1 as a mitochondrial matrix protein in contrast to a previous study suggesting Letmd1 as an outer mitochondrial membrane protein (Cho et al., 2007) (Q924L1, UniProt). Letmd1 is Letm1 domain containing 1 and Letm1 has two transmembrane domain and both termini are in the mitochondrial matrix (Lee et al., 2017) like Letmd1. Furthermore, Letm1 regulates mitochondrial swelling (Hasegawa et al., 2007), assembly of the respiratory chains (Tamai et al., 2008) and cristae organization (Nakamura et al., 2020) similar with Letmd1. Several studies report Letm1 (SLC55A1) to act as a K+/H+ exchanger (Froschauer et al., 2005) or Ca2+/H+ antiporter forming a hexamer with a cavity at the center (Shao et al., 2016). Further molecular and structural studies will be required to determine whether Letmd1 protein also functions as an ion transporter.

The mitochondrial matrix is the key locale for coordinate activity of OXPHOS complexes and Ucp1 protein-mediated uncoupling to maintain the thermogenic program of brown adipocytes. Interestingly, *Ucp1* knockout mice are reported to have impaired OXPHOS complex indicating a unique

interdependence between Ucp1 protein and OXPHOS function in BAT (Kazak et al., 2017). Similar to Ucp1 knockout mice, Letmd1-deficient BAT displays impaired expression of OXPHOS complex proteins and aberrant mitochondrial morphology leading to BAT dysfunction and cold intolerance. Taken together, we demonstrate that Letmd1 plays a critical role in regulating mitochondrial respiration that, in conjunction with UCP1, supports BAT thermogenic function.

Increasing the activity of BAT in humans is an emerging strategy to prevent obesity and metabolic disease by promoting energy expenditure (Chechi et al., 2014, Saito et al., 2014). Thus, newly identified molecular regulators of mitochondrial metabolism and BAT thermogenesis provide potential opportunities for prevention and therapeutic interventions for obesity (Kajimura et al., 2014, Hussain et al., 2020). Letmd1 is highly expressed in mature brown adipocytes and is dynamically regulated in response to environmental cues that signal thermogenic demand. Recently, PET/CT-guided fat biopsies study in humans show that LETMD1 is indeed a *bona fide* marker for brown adipocytes both in humans and mice (Perdikari et al., 2018). Therefore, the identification of Letmd1 advances our understanding of the specific mitochondrial mechanisms supporting BAT thermogenesis and implicate Letmd1 as a novel therapeutic target for the treatment of obesity and metabolic disease.

Materials And Methods

Cell culture, adipogenic differentiation and Oil-Red-O staining

An immortalized brown preadipocyte (iBPA) cell line was kindly provided by Dr. Shingo Kajimura (UCSF, San Francisco, CA, USA) and grown in high glucose Dulbecco's modified Eagle medium (DMEM, Gibco) containing 10% fetal bovine serum (Gibco) and 1% antibiotics at 37℃ in a humidified atmosphere with 5% CO_2. For brown adipocyte differentiation, cells were induced as previously described (Uldry et al., 2006).

Generation of stable overexpression or knockdown cell lines

To construct iBPA cells stably expressing FLAG-tagged mouse Letmd1, a retroviral infection system was used. For Letmd1 expression, DNA encoding the FLAG-tagged Letmd1 was inserted into the pRetroX-IRES-ZsGreen1 vector (Clontech Laboratories, Mountain View, CA, USA). For virus production, GP2-293 cells were transfected using TransIT®-LT1 Transfection Reagent (Mirus), and infected cells were selected using a FACSAria cell sorter (BD Biosciences) and maintained in high glucose Dulbecco's modified Eagle medium (DMEM) containing 10% fetal bovine serum (Gibco). To knockdown endogenous Letmd1 expression, we used a retrovirus-mediated shRNA system. Short-hairpin shRNAs were designed by selecting a target sequence for the mouse Letmd1 gene according to Knockout RNAi systems user manual (Clontech). The shRNA against Letmd1 was inserted into the multi-cloning site of the pSIREN-RetroQ-DsRed vector (Clontech). The following gene-specific sequences were used to successfully inhibit

Letmd1 expression: 5'-GATCCGCAACTGCTAGTCAAGCATTTCAAGAGAATGCTTGACTAGCAGTTGCTTTTTTG-3' and 5'-AATTCAAAAAAGCAACTGCTAGTCAAGCATTCTCTTGAAATGCTTGACTAGCAGTTGCG-3'. Control shRNA (scrambled) vector was provided by Clontech.

Animal experiments

ES cell clone (IKMC project: 84728) was purchased from EUCOMM based on the EUCOMM gene targeting strategy. The Letmd1 targeting allele contains a *lacZ* and a neomycin resistance gene cassette that is flanked by Flp recombinase target (FRT) sequences. This cassette was inserted into an intron between exon 2 and exon 3 of Letmd1 gene to disrupt endogenous Letmd1 expression. Exon 3 and exon 4 of Letmd1 gene are also flanked by loxP sites and there is a loxP site between the lacZ and neomycin resistance gene. Letmd1 heterozygous null mice (Letmd1 +/−) were obtained by microinjection of this ES cell clone into C57BL6/N mice (Macrogen). Methods to generate Matrix-APEX2 transgenic mice are described elsewhere (Park et al., 2021). Mice were maintained in a specific pathogen-free animal facility under institutional guidelines of the Korean Research Institute of Biotechnology and Bioscience, and all mouse experiments were approved and performed under institutional guidelines.

Indirect calorimetry

For indirect calorimetry studies, mice were housed individually in metabolic cages (CLAMS12, Columbus Instruments) with ad libitum access to food and water. Oxygen consumption rates and carbon dioxide production rates were measured for 48 hr. Activity was monitored simultaneously with metabolic measurements.

Core body temperature measurement and Infrared camera imaging

For measuring core temperature of cold exposed mice, mice were exposed 8°C in low temperature chamber (DHIN02-0034, DBL) and core body temperature was monitored using a rectal thermometer (Testo 925, Testo). The surface temperature of mice was measured with an infrared camera (Fortric 228, Fortric precision instruments) and analyzed with AnalyzIR (Fortric precision instruments) software.

Histology analysis

Mouse tissues were fixed in 10 % neutral buffered formalin (Sigma, HT501128) for 24 h and embedded in paraffin by an automated tissue processor (Leica, TP1020). 4 μm-thick tissue sections were obtained, deparaffinized, rehydrated, and stained with hematoxylin and eosin.

Extracellular flux assays

Oxygen consumption rate (OCR) was measured using Seahorse extracellular flux analyzer (Seahorse Bioscience). On the day before the experiment, the sensor cartridge was placed into the calibration buffer (Seahorse Bioscience) and incubated at 37°C in a non-CO_2 incubator. Prior to measurement, cells were equilibrated in assay medium containing 25 mM D-glucose, 4 mM L-glutamine and 1 mM sodium

pyruvate for 1 h. To measure OCR by mitochondrial respiration, cells were treated sequentially with 2.5 μM oligomycin, 5 μM Carbonyl cyanide m-chlorophenyl hydrazone (CCCP) and 2 μM rotenone/5 μM antimycin A. OCR was measured 1 h after 1 μM isoproterenol treatment. After the assays, the plates were saved, and protein levels were measured for each well to confirm equal cell numbers per well.

Biotin-phenol labeling in live cells.

APEX2-fusion constructs were introduced into HEK 293T, HEK AD or iBPA cells. In the case of iBPA cells, genes were introduced through electroporation, and Lipofectamine 2000 (Life Technologies) was used according to manufacturer protocols. After 18-24 h, the medium was changed to fresh growth medium containing 500 μM desthiobiotin-phenol (DBP). DBP-treated cells were incubated at 37°C under CO_2 for 30 min. Then, H_2O_2 was added to the cells for a final concentration of 1 mM H_2O_2, and the plate was gently agitated for 1 min at room temperature. The reaction was quenched by washing three times with ice-cold DPBS containing 5 mM trolox, 10 mM sodium ascorbate, and 10 mM sodium azide. Cells were then either lysed for western blot analysis or fixed for imaging analysis. Western blot analysis, fluorescence microscope imaging, and TEM imaging of DBP labelled cells were performed as described previously (Lee et al., 2016).

In situ biotinylation reaction of BAT from Matrix-APEX2 transgenic mice

BAT was harvested from Matrix-APEX2 transgenic mice and incubated with 500 μM desthiobiotin-phenol (DBP) in PBS for 1 h. Subsequently, diluted H_2O_2 (20 mM) was added to a final concentration of 2 mM H_2O_2 followed by gentle agitation for 2 min. The reaction was then quenched by adding DPBS containing 10 mM Trolox, 20 mM sodium azide, and 20 mM sodium ascorbate. Labeled BAT was homogenized using a FastPrep-24^{TM} bead homogenizer (MP Biomedicals) and lysed in RIPA buffer (Pierce) containing 1X protease inhibitor cocktail (GenDEPOT). Resulting lysates were sonicated on a Bioruptor (Cosmo Bio) for 15 min at 4°C and cleared by three rounds of centrifugation at 16,000 g for 20 min at 4°C. The clear supernatant was used for western blots.

Western blot analysis

Homogenized tissue or cells were lysed with ice-cold RIPA buffer (Pierce) containing 1X protease inhibitor cocktail (GenDEPOT) and incubated at 4°C for 30 min. After centrifugation at 13,000 rpm for 15 min, supernatant was moved to a new tube. Protein concentrations were measured using Bradford assay (Bio-Rad, Hercules, CA, USA). Protein samples were directly analyzed using sodium dodecyl sulfate - polyacrylamide gel electrophoresis (SDS-PAGE) with SDS sample buffer (60 mM Tris-Cl (pH 6.8), 10% sodium lauryl sulfate, 25% glycerol, 100 mM dithiothreitol, 0.04% Bromophenol blue) without boiling. Western blot analysis was performed according to standard methods. Antibodies used in immunoblot analyses included those against Letmd1 (LSBio); Ucp1 (Abcam); HSP90 (Santa Cruz); α-tubulin (Sigma-Aldrich); OXPHOS cocktail (Abcam); VDAC1 (Santa Cruz); COX- (Cell Signaling); GAPDH (Santa Cruz);

Lamin B1 (Abcam); streptavidin-HRP (Thermo Scientific); Mrpl39 (LSBio); Flag (Sigma-Aldrich); and Myc (Sigma-Aldrich).

mRNA expression analysis by qRT-PCR

Total RNA was extracted from tissue or cultured cells using TRIzol Reagent (Invitrogen) according to manufacturer instructions, and first-strand cDNA was synthesized from total RNA using the reverse transcriptase M-MLV and a random primer (Promega) according to manufacturer protocols. Real-time PCR was performed using 2X Real-time PCR Smart mix kit (SolGent) according to the manufacturer protocols. Gene expression levels were normalized to 60S ribosomal protein L32 (Rpl32).

Statistical analysis

All data are presented as mean ± s.e.m. The statistical significance of the comparisons was determined using Student's two-tailed t test.

References

1. Blondin, D. P., Labbé, S. M., Tingelstad, H. C., Noll, C., Kunach, M., Phoenix, S., … Haman, F. (2014). Increased brown adipose tissue oxidative capacity in cold-acclimated humans. *The Journal of Clinical Endocrinology & Metabolism*, *99*(3), E438-E446.
2. Bowman, T. A., O'Keeffe, K. R., D'Aquila, T., Yan, Q. W., Griffin, J. D., Killion, E. A., … Greenberg, A. S. (2016). Acyl CoA synthetase 5 (ACSL5) ablation in mice increases energy expenditure and insulin sensitivity and delays fat absorption. *Molecular metabolism*, *5*(3), 210–220.
3. Calvo, S. E., Clauser, K. R., & Mootha, V. K. (2016). MitoCarta2.0: an updated inventory of mammalian mitochondrial proteins. *Nucleic acids research*, *44*(D1), D1251-D1257.
4. Chechi, K., Nedergaard, J., & Richard, D. (2014). Brown adipose tissue as an anti-obesity tissue in humans. *Obesity Reviews*, *15*(2), 92–106.
5. Cho, G. W., Shin, S. M., Kim, H. K., Ha, S. A., Kim, S., Yoon, J. H., … Kim, J. W. (2007). HCCR-1, a novel oncogene, encodes a mitochondrial outer membrane protein and suppresses the UVC-induced apoptosis. *BMC Cell Biology*, *8*(1), 1–12.
6. Chondronikola, M., Volpi, E., Børsheim, E., Porter, C., Annamalai, P., Enerbäck, S., … Sidossis, L. S. (2014). Brown adipose tissue improves whole-body glucose homeostasis and insulin sensitivity in humans. *Diabetes*, *63*(12), 4089–4099.
7. Floyd, B. J., Wilkerson, E. M., Veling, M. T., Minogue, C. E., Xia, C., Beebe, E. T., … Pagliarini, D. J. (2016). Mitochondrial protein interaction mapping identifies regulators of respiratory chain function. *Molecular cell*, *63*(4), 621–632.
8. Forner, F., Kumar, C., Luber, C. A., Fromme, T., Klingenspor, M., & Mann, M. (2009). Proteome differences between brown and white fat mitochondria reveal specialized metabolic functions. *Cell metabolism*, *10*(4), 324–335.

9. Froschauer, E., Nowikovsky, K., & Schweyen, R. J. (2005). Electroneutral K+/H+ exchange in mitochondrial membrane vesicles involves Yol027/Letm1 proteins. *Biochimica et Biophysica Acta (BBA)-Biomembranes*, *1711*(1), 41–48.
10. Fukasawa, Y., Tsuji, J., Fu, S. C., Tomii, K., Horton, P., & Imai, K. (2015). MitoFates: Improved Prediction of Mitochondrial Targeting Sequences and Their Cleavage Sites*[S]. *Molecular & Cellular Proteomics*, *14*(4), 1113–1126.
11. Hasegawa, A., & van der Bliek, A. M. (2007). Inverse correlation between expression of the Wolfs Hirschhorn candidate gene Letm1 and mitochondrial volume in C. elegans and in mammalian cells. *Human molecular genetics*, *16*(17), 2061–2071.
12. Hung, V., Zou, P., Rhee, H. W., Udeshi, N. D., Cracan, V., Svinkina, T., … Ting, A. Y. (2014). Proteomic mapping of the human mitochondrial intermembrane space in live cells via ratiometric APEX tagging. *Molecular cell*, *55*(2), 332–341.
13. Hung, V., Lam, S. S., Udeshi, N. D., Svinkina, T., Guzman, G., Mootha, V. K., … Ting, A. Y. (2017). Proteomic mapping of cytosol-facing outer mitochondrial and ER membranes in living human cells by proximity biotinylation. *elife*, *6*, e24463.
14. Hussain, M. F., Roesler, A., & Kazak, L. (2020). Regulation of adipocyte thermogenesis: mechanisms controlling obesity. *The FEBS journal*, *287*(16), 3370–3385.
15. Kajimura, S., & Saito, M. (2014). A new era in brown adipose tissue biology: molecular control of brown fat development and energy homeostasis. *Annual review of physiology*, *76*, 225–249.
16. Kazak, L., Chouchani, E. T., Stavrovskaya, I. G., Lu, G. Z., Jedrychowski, M. P., Egan, D. F., … Spiegelman, B. M. (2017). UCP1 deficiency causes brown fat respiratory chain depletion and sensitizes mitochondria to calcium overload-induced dysfunction. *Proceedings of the National Academy of Sciences*, *114*(30), 7981-7986.
17. Klingenberg, M. (1990). Mechanism and evolution of the uncoupling protein of brown adipose tissue. *Trends in biochemical sciences*, *15*(3), 108–112.
18. Krogh, A., Larsson, B., Von Heijne, G., & Sonnhammer, E. L. (2001). Predicting transmembrane protein topology with a hidden Markov model: application to complete genomes. *Journal of molecular biology*, *305*(3), 567–580.
19. Labbé, S. M., Caron, A., Bakan, I., Laplante, M., Carpentier, A. C., Lecomte, R., & Richard, D. (2015). In vivo measurement of energy substrate contribution to cold-induced brown adipose tissue thermogenesis. *The FASEB Journal*, *29*(5), 2046–2058.
20. Lee, S. Y., Kang, M. G., Park, J. S., Lee, G., Ting, A. Y., & Rhee, H. W. (2016). APEX fingerprinting reveals the subcellular localization of proteins of interest. *Cell reports*, *15*(8), 1837–1847.
21. Lee, S. Y., Kang, M. G., Shin, S., Kwak, C., Kwon, T., Seo, J. K., … Rhee, H. W. (2017). Architecture mapping of the inner mitochondrial membrane proteome by chemical tools in live cells. *Journal of the American Chemical Society*, *139*(10), 3651–3662.
22. Liu, X., Wang, S., You, Y., Meng, M., Zheng, Z., Dong, M., … Jin, W. (2015). Brown adipose tissue transplantation reverses obesity in Ob/Ob mice. *Endocrinology*, *156*(7), 2461–2469.

23. Marcher, A. B., Loft, A., Nielsen, R., Vihervaara, T., Madsen, J. G. S., Sysi-Aho, M., … Mandrup, S. (2015). RNA-seq and mass-spectrometry-based lipidomics reveal extensive changes of glycerolipid pathways in brown adipose tissue in response to cold. *Cell reports*, *13*(9), 2000–2013.
24. Martell, J. D., Deerinck, T. J., Sancak, Y., Poulos, T. L., Mootha, V. K., Sosinsky, G. E., … Ting, A. Y. (2012). Engineered ascorbate peroxidase as a genetically encoded reporter for electron microscopy. *Nature biotechnology*, *30*(11), 1143–1148.
25. Mo, Q., Salley, J., Roshan, T., Baer, L. A., May, F. J., Jaehnig, E. J., … Chen, M. H. (2017). Identification and characterization of a supraclavicular brown adipose tissue in mice. *JCI insight*, *2*(11).
26. Nakamura, S., Matsui, A., Akabane, S., Tamura, Y., Hatano, A., Miyano, Y., … Oka, T. (2020). The mitochondrial inner membrane protein LETM1 modulates cristae organization through its LETM domain. *Communications biology*, *3*(1), 1–11.
27. Pagliarini, D. J., Calvo, S. E., Chang, B., Sheth, S. A., Vafai, S. B., Ong, S. E., … Mootha, V. K. (2008). A mitochondrial protein compendium elucidates complex I disease biology. *Cell*, *134*(1), 112–123.
28. Park, I., Kim, K., Kim, J., Bae, S., Jung, M., … Rhee, H.W. (2021). In vivo mitochondrial matrix proteome profiling reveals RTN4IP1/OPA10 as an antioxidant NADPH oxidoreductase. *bioRxiv*, 10.1101/2021.10.14.464368.
29. Perdikari, A., Leparc, G. G., Balaz, M., Pires, N. D., Lidell, M. E., Sun, W., … Wolfrum, C. (2018). BATLAS: deconvoluting brown adipose tissue. *Cell reports*, *25*(3), 784–797.
30. Rath, S., Sharma, R., Gupta, R., Ast, T., Chan, C., Durham, T. J., … Mootha, V. K. (2021). MitoCarta3.0: an updated mitochondrial proteome now with sub-organelle localization and pathway annotations. *Nucleic acids research*, *49*(D1), D1541-D1547.
31. Rhee, H. W., Zou, P., Udeshi, N. D., Martell, J. D., Mootha, V. K., Carr, S. A., & Ting, A. Y. (2013). Proteomic mapping of mitochondria in living cells via spatially restricted enzymatic tagging. *Science*, *339*(6125), 1328–1331.
32. Saito, M. (2014). Human brown adipose tissue: regulation and anti-obesity potential. *Endocrine journal*, *61*(5), 409–416.
33. Shao, J., Fu, Z., Ji, Y., Guan, X., Guo, S., Ding, Z., … Shen, Y. (2016). Leucine zipper-EF-hand containing transmembrane protein 1 (LETM1) forms a Ca 2+/H+ antiporter. *Scientific reports*, *6*(1), 1–9.
34. Stanford, K. I., Middelbeek, R. J., Townsend, K. L., An, D., Nygaard, E. B., Hitchcox, K. M., … Goodyear, L. J. (2012). Brown adipose tissue regulates glucose homeostasis and insulin sensitivity. *The Journal of clinical investigation*, *123*(1).
35. Tamai, S., Iida, H., Yokota, S., Sayano, T., Kiguchiya, S., Ishihara, N., … Oka, T. (2008). Characterization of the mitochondrial protein LETM1, which maintains the mitochondrial tubular shapes and interacts with the AAA-ATPase BCS1L. *Journal of cell science*, *121*(15), 2588–2600.
36. Uldry, M., Yang, W., St-Pierre, J., Lin, J., Seale, P., & Spiegelman, B. M. (2006). Complementary action of the PGC-1 coactivators in mitochondrial biogenesis and brown fat differentiation. *Cell metabolism*, *3*(5), 333–341.

37. Yoneshiro, T., Aita, S., Matsushita, M., Kayahara, T., Kameya, T., Kawai, Y., … Saito, M. (2013). Recruited brown adipose tissue as an antiobesity agent in humans. *The Journal of clinical investigation*, *123*(8), 3404–3408.

Declarations

Acknowledgments

We gratefully acknowledge Hye-Young Um, Hee-Saeng Jung and Ju Eun Kim for administrative and technical support. We thank Shingo Kajimura for providing iBPA cells and Hail Kim, Seyun Kim and Min-Woo Lee for providing reagents and helpful discussion. This work was supported by the KRIBB and the National Research Foundation of Korea (2021R1A2C200757311, 2020R1A2C2007111, 2019R1A2C1006035).

Author Contributions

A.P, K.K, W.K.K, K.-H.B and J.M.S conceived the study and interpreted data. A.P, K.K and I.P performed experiments. A.P, K.K, W.K.K, K.-H.B and J.M.S wrote the manuscript. D.-S.K, J.K, D.-S.L, J.Y.M, H.-W.R, E.-J.W, K.-J.O, E.W.L, B.S.H and S.C.L critically reviewed the study and provided helpful discussion. All authors read and approved the final version of the manuscript.

Declaration of Interests

The authors declare no competing financial interests.

Figures

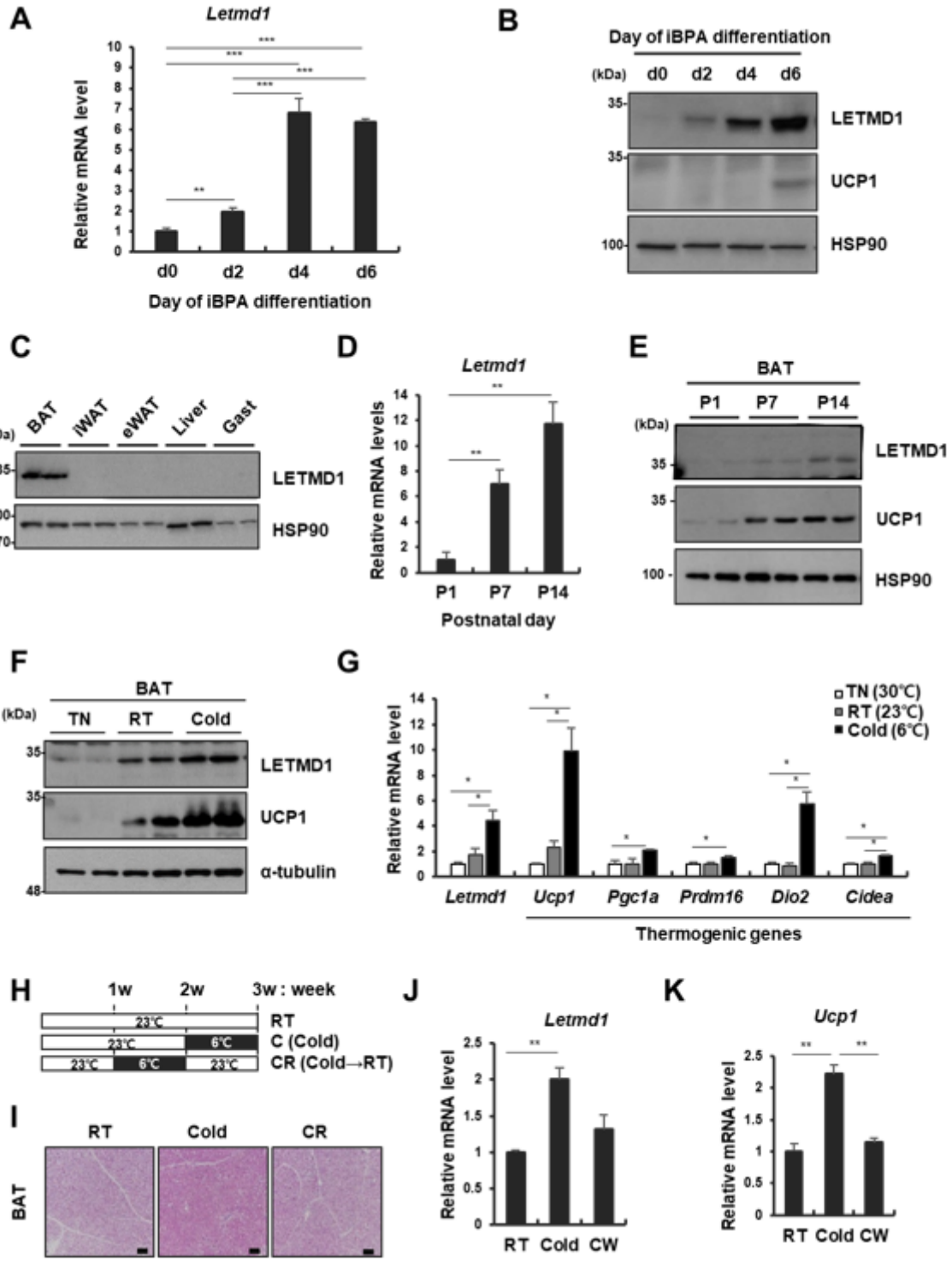

Figure 1

The Letmd1 gene encodes a brown adipocyte-enriched and cold-inducible protein (A) mRNA expression of Letmd1 during brown adipocyte (iBPA) differentiation. Expression is normalized to Rpl32. (B) Western blots of Letmd1 and Ucp1 protein during brown adipocyte (iBPA) differentiation. (C) Western blots of Letmd1 protein in brown adipose tissue (BAT), inguinal white adipose tissue (iWAT), epididymal white adipose tissue (eWAT), liver, and gastrocnemius muscle (Gast). HSP90 is loading control. (D) mRNA

expression of Letmd1 from perinatal BAT. (E) Western blots of Letmd1 and Ucp1 protein in BAT from postnatal day 1 (P1), day 7 (P7) and day 14 (P14) mice. (F) Representative western blots of Letmd1 and Ucp1 protein in BAT from mice after 5 days exposure to TN (thermoneutral, 30℃), RT (room temperature, 23℃) and Cold (6℃). (G) mRNA expression of Letmd1 and thermogenic genes in same sets as in (F). Expression is normalized to Rpl32. (H) Experimental scheme for cold challenge. (I) H&E staining of BAT sections from mice exposed to cold (6℃) and mice adapted to room temperature (23℃) after cold stimulation. Scale bar, 200 μm. (J, K) mRNA expression of Letmd1 and Ucp1 in same sets as in (H). Expression is normalized to Rpl32. n=3 mice per group. Data presented as mean ± s.e.m. *p < 0.05, ** p < 0.005, *** p < 0.0005

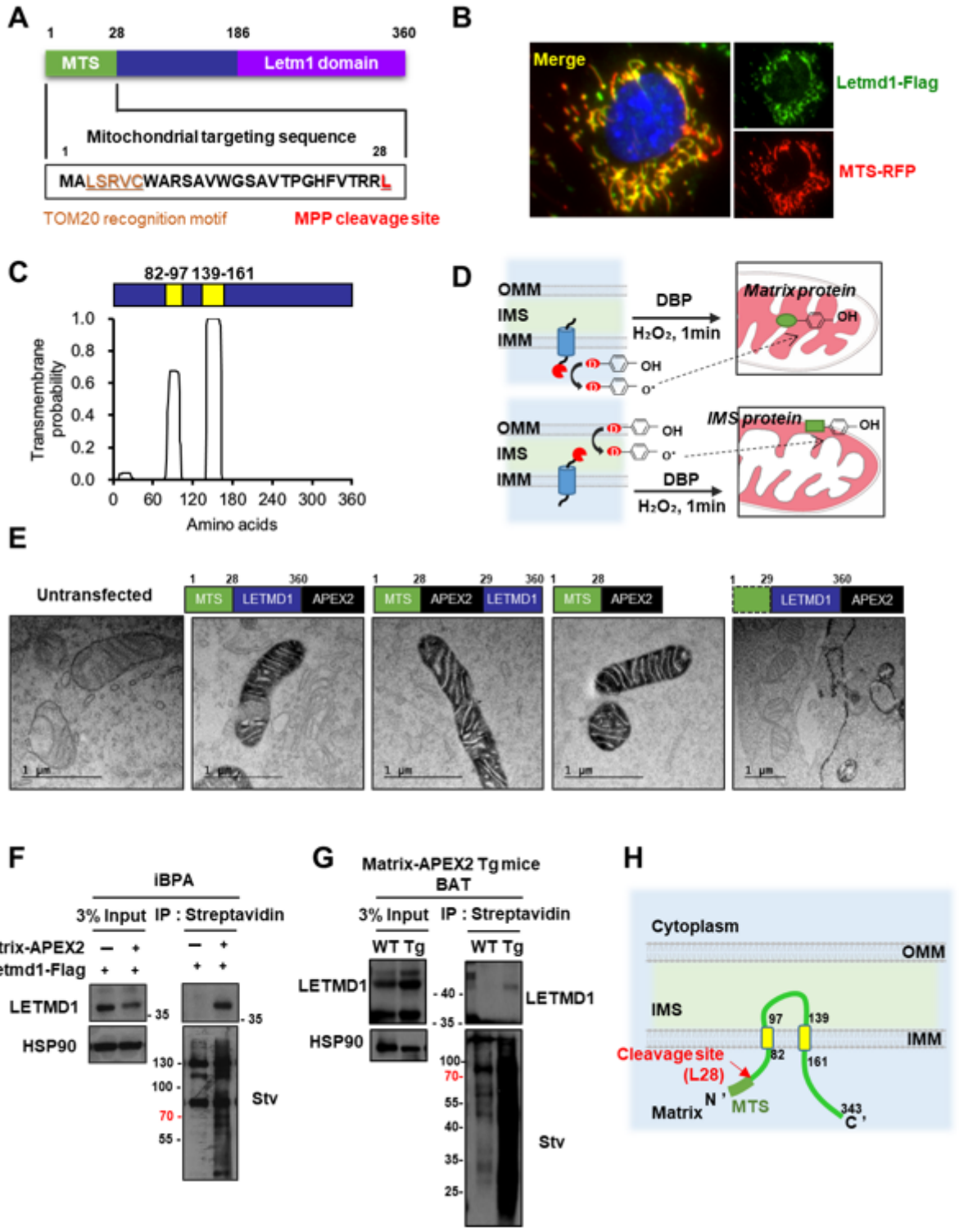

Figure 2

Letmd1 is a mitochondrial matrix protein (A) Identification of a putative mitochondrial targeting sequence (MTS) and cleavage site for human LETMD1 with MitoFates analysis. (B) Immunofluorescence image of LETMD1-Flag (Green), mitochondria (Red) and DAPI (Blue) in brown adipocytes differentiated from iBPA cells. (C) TMHMM analysis of human LETMD1 protein sequence revealing two transmembrane domains (yellow boxes). (D) Experimental scheme of proximity labeling using APEX2 localized to the

mitochondrial matrix (top) or intermembrane space (bottom). APEX2 enzyme (red) labels compartment-specific proteomes using desthiobiotin-phenol (D, DBP) as a substrate. Outer mitochondrial membrane, OMM; Intermembrane space, IMS; Inner mitochondrial membrane, IMM. (E) Electron micrographs of APEX2 staining patterns in untransfected HEK 293 cells and HEK 293 cells transfected with MTS-Letmd1-APEX2 (C-terminus fusion), MTS-APEX2-Letmd1 (N-terminus fusion), MTS-APEX2, and ΔMTS-Letmd1-APEX2 expression constructs. Scale bar, 1 μm. (F) Western blot of Letmd1 protein and matrix-APEX2 biotinylated proteins (Stv; streptavidin-HRP) in mature brown adipocytes. HSP90 is loading control. (G) Western blots of Letmd1 protein and matrix-APEX2 biotinylated proteins (Stv; streptavidin-HRP) in BAT lysates from Matrix-APEX2 transgenic mice. (H) Proposed topology of Letmd1. Transmembrane domain (yellow), MTS (green) and MTS cleavage site (arrow) are depicted.

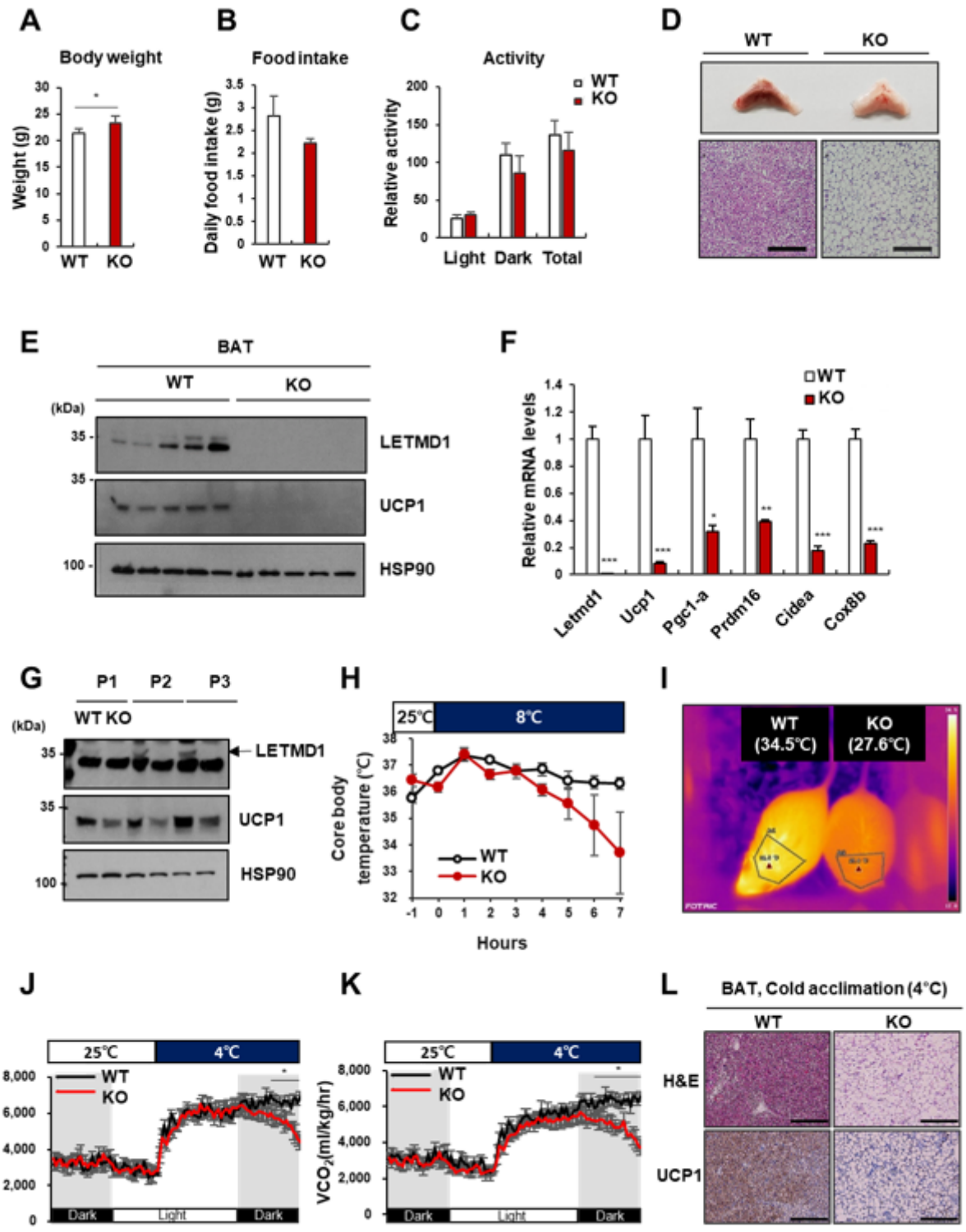

Figure 3

Letmd1 is required for adaptive thermogenesis (A-C) Body weight, food intake and locomotor activity of 13-week-old WT and Letmd1 KO mice. n=4 per group. (D) Gross image of brown adipose tissue (BAT) and H&E stained BAT tissue sections. Scale bar, 200 μm. (E) Western blots of Letmd1 and Ucp1 protein in BAT of 13-week-old mice (F) mRNA expression of Letmd1 and brown adipocyte marker genes. Expression is normalized to Rpl32. (G) Western blots of Letmd1 and Ucp1 protein in BAT from postnatal day 1 (P1), day

2 (P2), and day 3 (P3) (H) Core body temperature of mice during cold (8℃) challenge. (I) Infrared thermography of mice in (H) at 5 h cold challenge. (J, K) Oxygen consumption rates and carbon dioxide production rates of mice exposed to cold (4℃). (L) Representative H&E staining and Ucp1 protein immunostaining of BAT from WT and Letmd1 KO mice exposed to cold (4℃) for 5 h. Scale bar, 200 μm. n = 4-5 mice per group. Data presented as mean ± s.e.m. *p < 0.05, ** p < 0.005, *** p < 0.0005

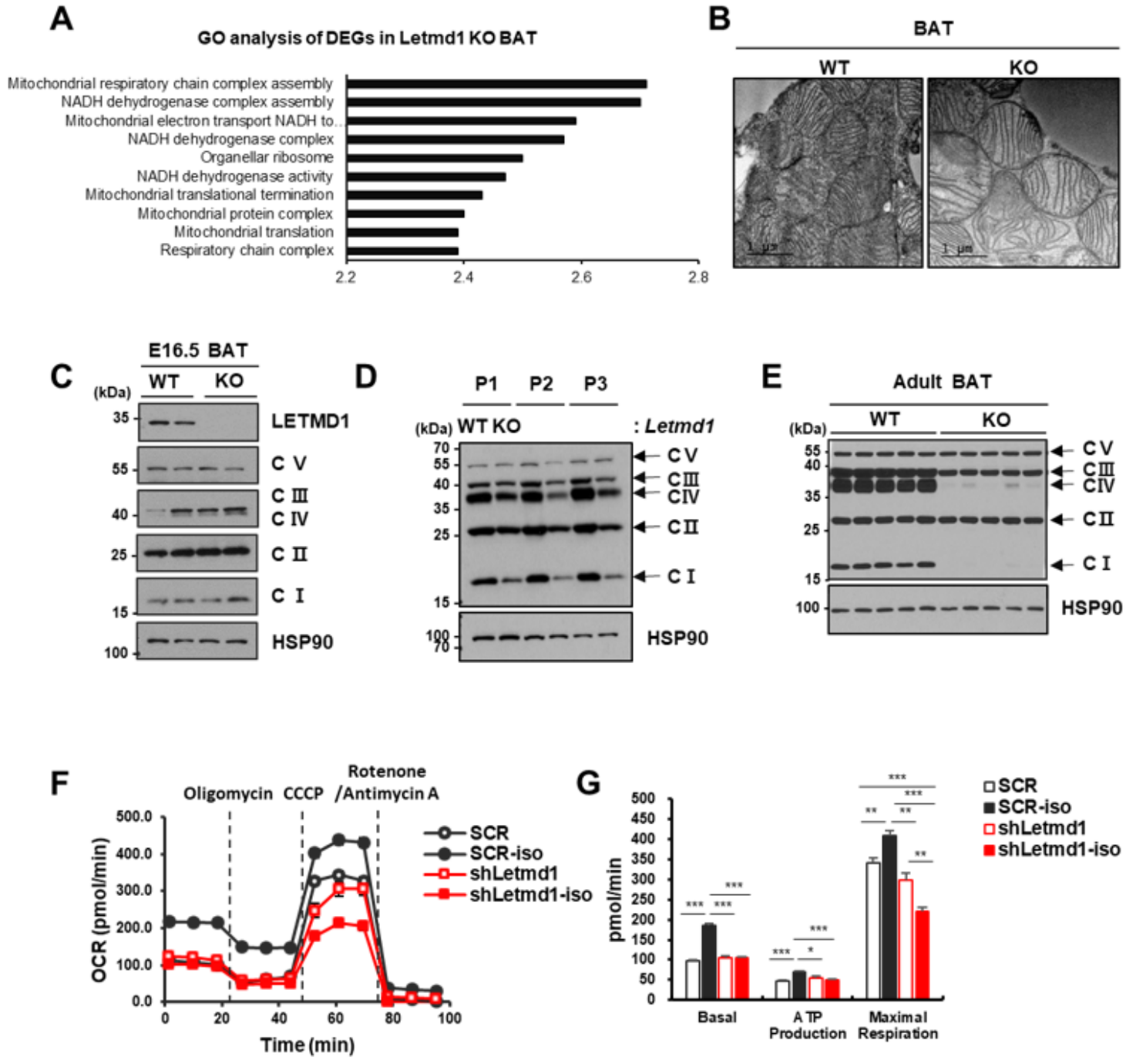

Figure 4

Letmd1 is supports mitochondrial respiration of stimulated brown adipocytes (A) Gene ontology analysis of BAT transcriptomes from WT and Letmd1 KO mice. n=3 per group. (B) Electron micrographs of BAT

showing mitochondrial structure. Scale bar, 1 μm. (C) Western blots of OXPHOS complex and Letmd1 proteins from E16.5 embryonic BAT. (D) Western blots of OXPHOS complex proteins from perinatal BAT. (E) Western blots of OXPHOS complex proteins from adult BAT. (F) Oxygen consumption rates of control (SCR) and Letmd1 knockdown (shLetmd1) brown adipocytes differentiated from iBPA cells in response to 1 h pre-treatment of 1 μM isoproterenol (iso). (G) Basal respiration, ATP production and maximal respiration in same sets as (F). Data presented as mean ± s.e.m. *p < 0.05, ** p < 0.005, *** p < 0.0005

Supplementary Files

This is a list of supplementary files associated with this preprint. Click to download.

- Parketalsupplementaryfiles110321NatureComm.docx